Comparison of photon-beams scans on 3D-positioning CZT with a defect-enabled numerical simulation.

Alexandre Delcourt[1], Guillaume Montémont[1], Anthony Schaal[1].

1 CEA Leti, Université Grenoble Alpes, F-38000 Grenoble, France.

I. Context and motivations

Context

- Gamma Imaging: Localization or identification of a gamma-emitting radioactive source with a sensing material.
- CZT : semiconductor frequently used due to its good physical properties (life time constant and mobility of charge carriers.

Fig 1. Gamma camera used for security.

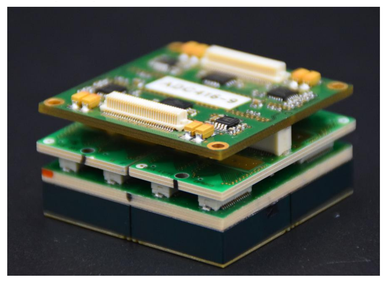

Fig 2. CZT Detector with the electronics.

- **Problem :** Presence of structural defects appearing during crystal growth and disturbing the charge collection and the localization of interactions (Fig 4,5).

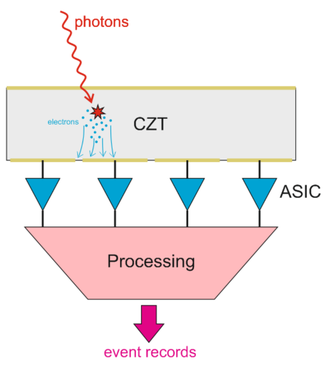

Fig 3. CZT detector functioning.

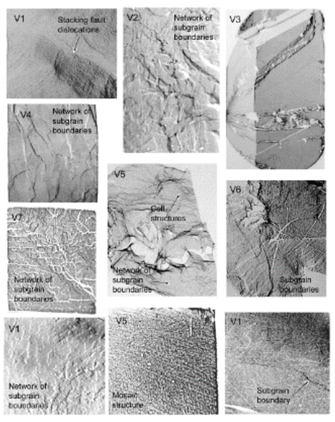

Fig 4. Illustration of some defects [2].

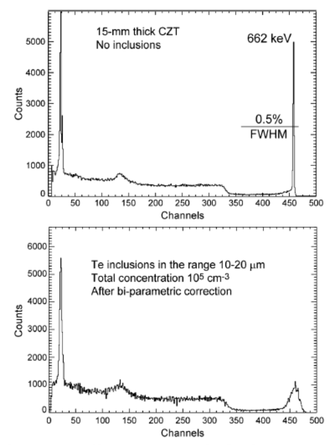

Fig 5. Influence of defects on the energy spectrum of Cs^{137} [2].

Motivations

- Understand the influence of structural defects of CZT using simulations.
- Find a coherence and retrieve the internal structure of the actual crystal by modifying the parameters of the simulation.

II. 3D Positioning

Sub-pixelation

- 3D positioning using the pixel affected and its neighbours to refine the X and Y values.
- Use of both cathode and anode signal to estimate the depth value.

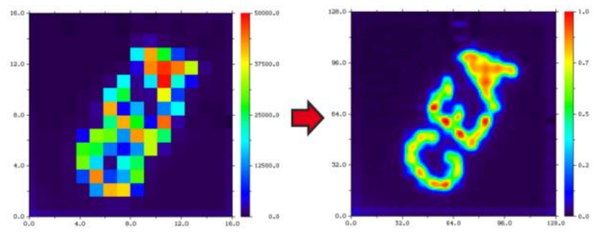

Fig 6. Effect of sub-pixelation on position estimation.

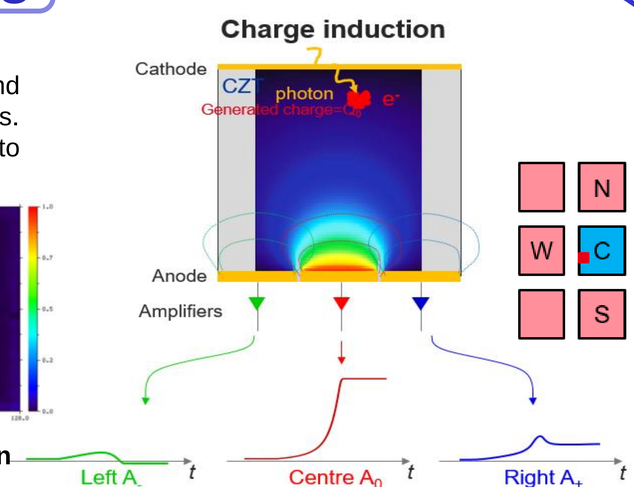

Fig 7. Sub-pixelation using induced signals.

MLEM (Maximum Likelihood Expectation Maximization)

- Algorithm more accurate than centre of mass to compute positioning.
- Separable analytical model Based on CIE (Charge Induction Efficiency).
- $CIE(x,y,z) \approx f\left(\frac{g(x)+g(y)}{h(z)}\right)$.
- Bias appearing due to variable separation.

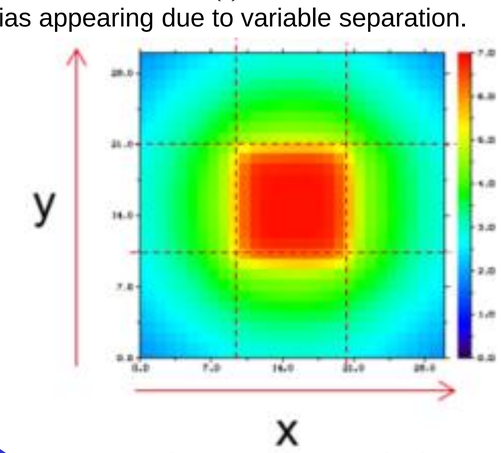

Fig 8. CIE on 3x3 pixels.

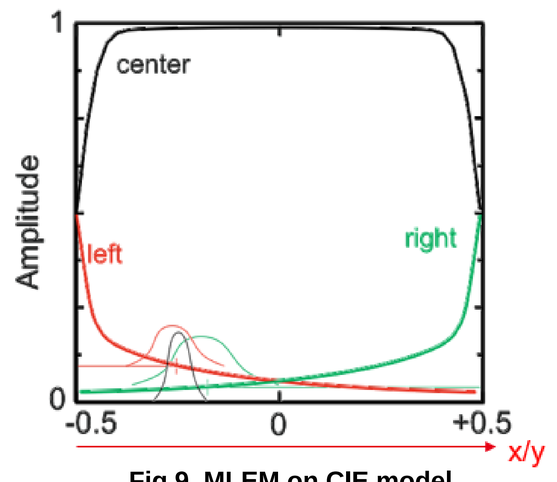

Fig 9. MLEM on CIE model.

III. 3D Simulation including defects

3D Simulation

- Use of the C++ modelling environment Tasmania for the detector and particle physics.
- Update of the electric field with the evaluation of trapped charge density ($\Delta V = \frac{\rho}{\epsilon}$).

Implementation of realistic defects

- Different types of defects.
  - Randomly distributed points defects (1).
  - Plane defect (2).
  - Highly conductive spherical defect (3).
  - Intense localized X-ray irradiation (4).

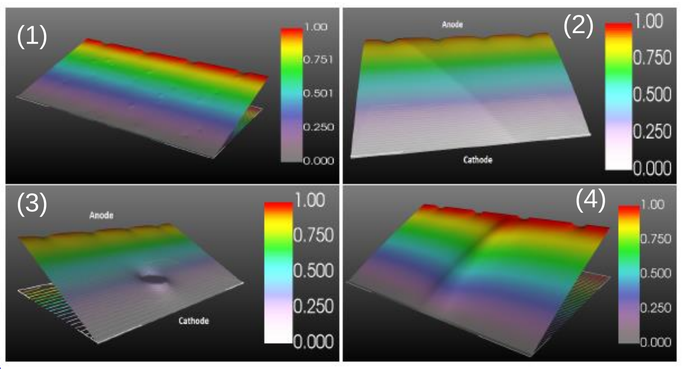

Fig 10. Slices of simulated applied potentials in the detector for different defects.

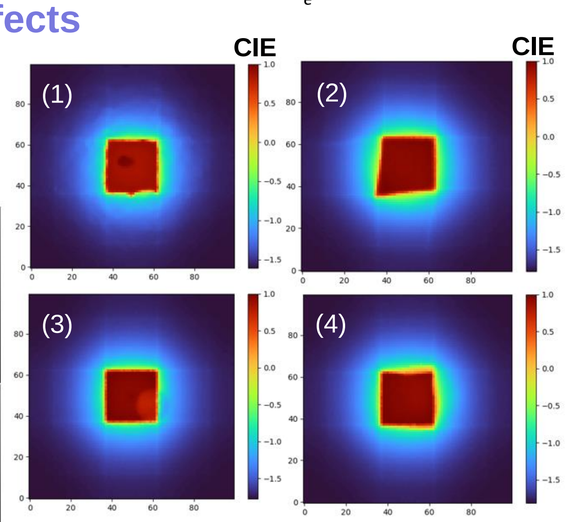

Fig 11. Simulated 2D CIE for different defects.

IV. Experimental measures

Experimental bench

- CZT detector coupled to translation bench with an amplitude of 25 cm (Fig 12).
- XY scan of the detector using the translation bench driven by LabView.
- For each interaction, extraction of the cathode and anode induced signals for the collecting pixel and its 8 direct neighbours using 2 shaped amplitudes per pixel.

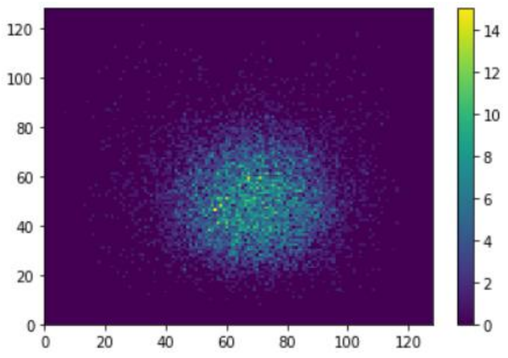

Fig 13. 2D Histogram of the XY position after a pixel scan with a collimated source. Scale : 128 ⇔ 2,46 mm. Co^{57} source with a 900 µm tungsten collimator.

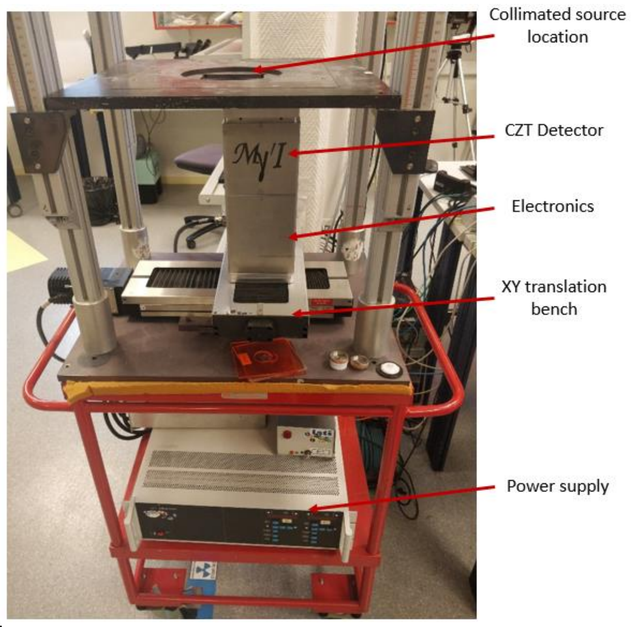

Fig 12. Picture of the experimental bench for XY scans.

Data acquisition and processing

- Output data : amplified induced signals on the collecting anodes and the adjacent ones.
- 2D CIE mapping of the detector processing the data under Tasmania and Python by dividing the induced charge by the initial deposited charge of the photon interaction estimated by the electronics.

V. Comparison real/simulated data

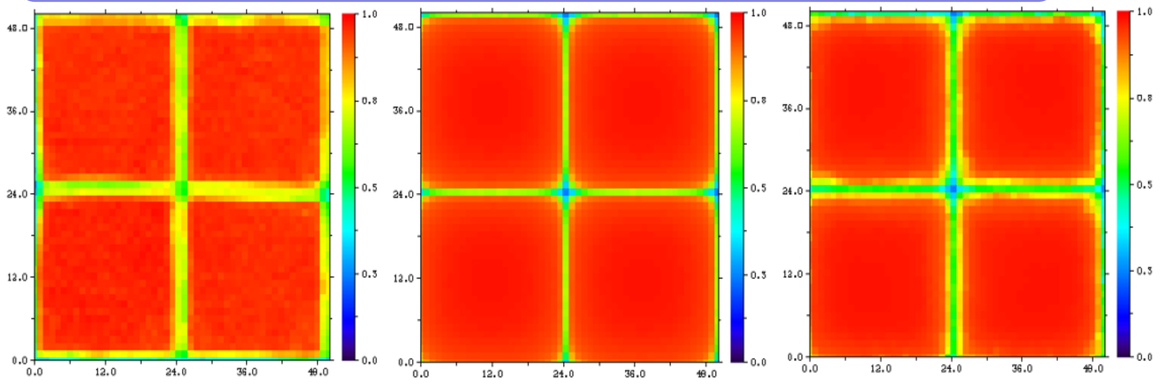

Fig 14. CIE maps of a 2x2 adjacent anodes from different data. From left to right : experimental data from a XY scan, idealized simulation and simulation including defects to model experimental data.

- CIE mapping for different types of data (Fig 14) to compare collection performances between simulation and experimental data.
- The addition of defects in the simulation impairs the collection especially on the edges of the electrodes (impact on charge sharing due to the field lines curves).
- Possible to approach the experimental map adding defects in the simulation by modifying the parameters (applied potential, conductivity, localized charge traps).

VI. Conclusion and prospects

Conclusion

- The simulations allow to observe quickly the influence of defects on the charge collection of a CZT detector.
- By comparing the experimental and simulated data we can observe the differences on the CIE maps and find the areas of the crystal the more concerned by the defects.
- The modification of the parameters of the simulation as the applied potential or the type/position/intensity/size of the defects brings closer to reality.

Prospects

- Approach the internal structure of a CZT detector to have better knowledge of its defects and their influence on the charge collection and electric field curves without realizing a time-consuming calibration which may take hours.
- Correct the output signal to have a better estimation of the interaction position and improve the performance of the detector.

References

[1] G. Montémont, S. Lux, O. Monnet, S. Stanchina and L. Verger, *Studying spatial resolution of CZT detectors using sub-pixel positioning for SPECT, IEEE Trans. Nucl. Sci.* **61** (2014) 2559.

[2] A.E. Bolotnikov, S. Babalola, G.S. Camarda, Y. Cui, R. Gul, S.U. Egarievwe et al., *Correlations Between Crystal Defects and Performance of CdZnTe Detectors, IEEE Trans. Nucl. Sci.* **58** (2011) 1972.

[3] A. Delcourt, G. Montémont, *GPU-accelerated CZT detector simulation with charge build-up effects, 2023 JINST* ***18*** *P02005*.